Robust and efficient solution of the 2D shallow water equation with domains containing dry beds

Stephen Roberts* Christopher Zoppou†

(Received 7 August 2000)

Abstract

A number of the standard numerical methods used to solve the two-dimensional shallow water wave equations are unstable if their

*Research School of Information Science and Engineering, Australian National University, Canberra, ACT 0200, Australia.

†CSIRO Land and Water, Canberra, Water Division, ACTEW Corporation, Canberra, Australia.

[0]See http://anziamj.austms.org.au/V42/CTAC99/Robe for this article and ancillary services, Published 27 Nov 2000.

domains contain dry beds. We present a robust and stable finite volume method based on an unstructured triangular grid which can deal with dry beds. In particular we present a second-order explicit method which deal with dry beds in a stable manner. The method uses a simple approximate one dimensional Riemann solver due to Toro which provides the basis for an efficient implementation.

Contents

1 Introduction

The shallow water equations are used extensively to model the behaviour of flows produced by precipitation or as a result of the failure of man-made structures. These problems generally involve sudden releases of water or intense rainfall bursts which produce rapid runoff. Both problems are characterised by abrupt changes in water depth and flow rates. In addition, these phenomena also involve water flowing over dry terrain, see for example Zoppou and Roberts [18]. Models which can accurately and efficiently simulate the behaviour of abrupt flows over a dry bed are required. A two-dimensional model which is capable of simulating abrupt changes in flow is described. The finite volume model is efficient and is capable of simulating flows over a dry bed. It has second-order accuracy and uses an approximate Riemann solver to solve the shallow water equations on an unstructured triangular grid. The method uses a simple approximate one dimensional Riemann solver due to Toro [13] which provides the basis for an efficient implementation.

2 Shallow Water Equation

The conservative form of the two-dimensional shallow water equations are given by [15]

$$\frac{\partial \mathbf{U}}{\partial t} + \nabla \cdot \mathbf{F} = \mathbf{0} \tag{1}$$

where (and through out) $\mathbf{U}$ is a vector of conservative variables: h, height; u, x "momentum"; and v, y "momentum", and $\mathbf{F}$ is the flux tensor. It can be expressed in Cartesian form as

$$\frac{\partial \mathbf{U}}{\partial t} + \frac{\partial \mathbf{G}}{\partial x} + \frac{\partial \mathbf{H}}{\partial y} = \mathbf{0} \tag{2}$$

where $\mathbf{G}$ and $\mathbf{H}$ are the Cartesian components of $\mathbf{F}$. The vectors $\mathbf{U}$, $\mathbf{G}$ and $\mathbf{H}$ can be expressed in terms of the primary variables, u, v and h as

$$\mathbf{U} = \begin{bmatrix} h \\ uh \\ vh \end{bmatrix}, \quad \mathbf{G} = \begin{bmatrix} uh \\ u^2h + gh^2/2 \\ uvh \end{bmatrix} \text{ and } \mathbf{H} = \begin{bmatrix} vh \\ uvh \\ v^2h + gh^2/2 \end{bmatrix} \tag{3}$$

in which g is the acceleration due to gravity, h is the water depth and u and v are the flow velocity in the x and y-directions respectively. The system is strictly hyperbolic with three real and distinct eigenvalues.

3 Numerical Solution of the Shallow Water Equation

It is the hyperbolic character of the shallow water equations that makes finding solutions to these equations difficult. Hyperbolic equations admit discontinuous and smooth solutions. Even for the case in which the initial conditions are smooth, the non-linear character combined with the hyperbolic type of the equations can lead to discontinuous solutions in finite time. The non-linear character of the shallow water equations means that analytical solutions to these equations are limited to only very special cases. Numerical methods are generally used to obtain solutions to practical problems.

Local initial value problems which involve discontinuous neighbouring states are known as the *Riemann* problems. Numerical schemes based on the solution of local Riemann problems are generally known as Godunov-type schemes. Their main advantages are that they are robust and accurately capture the location of discontinuities such as shocks and contact surfaces. Two-dimensional Riemann solvers do not appear to have matured enough to be used in the construction of multi-dimensional schemes. Even if such solvers were available, the resulting schemes are likely to be too complicated for common use [3]. A number of efficient one-dimensional approximate Riemann solvers have been proposed [9], [4], [5], [3]. These can be used to solve the two-dimensional dam break problem on a Cartesian grid using *fractional step* or *splitting techniques* [11]. The Finite Volume Method can also be used to solve the two-dimensional problem [17], [1]. Like finite elements,

the major advantage of the finite volume method is that it can be applied to any unstructured grid. Generally, the finite volume method requires less computational effort than finite elements because it involves the solution of a local one-dimensional Riemann problem, which can be solved efficiently.

From our experience with numerical schemes for solving the dam break problem, the *approximate Riemann solver* developed by Toro [12] was found to be robust and efficient. Unlike many other schemes, such as finite differences and other approximate Riemann solvers, it avoids the problems associated with sonic points, where a non-physical expansive shock is produced. The finite volume method and the approximate Riemann solver developed by Toro [12] have been chosen to solve the shallow water equations in two-dimensions.

4 Finite Volume Method

The finite volume method is based on the integral form of the conservation equation (2). The discretisation of the integral form of (2) ensures that the basic quantities, mass and momentum will also be conserved across a discontinuity [6]. Integrating (2) over an arbitrary triangular element E_i, the basic equation of the finite volume method obtained using the divergence

theorem is given by

$$\frac{\partial}{\partial t}\int_{E_i}\mathbf{U}\,dA+\oint_{\partial E_i}\mathbf{F}\cdot\mathbf{n}\,dS=0 \tag{4}$$

in which $\mathbf{n}$ is the unit outward vector normal to the boundary S_i, and dA and dS are the area and arc elements respectively. This law states that the time rate of change in $\mathbf{U}$ inside a control volume E_i, depends on the total flux through the boundary ∂A_i. The integrand $\mathbf{F}\cdot\mathbf{n}$ is the normal flux across a surface with normal $\mathbf{n}$.

Consider the rotation matrix

$$\mathbf{T_n}=\begin{bmatrix}1&0&0\\0&n_1&n_2\\0&-n_2&n_1\end{bmatrix} \tag{5}$$

where $\mathbf{n}=(n_1,n_2)$. The application of the rotation matrix $\mathbf{T_n}$ aligns the normal, $\mathbf{n}$ with the x-axis. Using the *rotational invariance* property of the two-dimensional shallow water equations,

$$\mathbf{F}(\mathbf{U})\cdot\mathbf{n}=\mathbf{T_n}^{-1}\mathbf{G}(\mathbf{T_n}\mathbf{U}). \tag{6}$$

Using (6), (4) becomes

$$\frac{\partial}{\partial t}\int_{E_i}\mathbf{U}\,dA+\oint_{\partial E_i}\mathbf{T_n}^{-1}\mathbf{G}(\mathbf{T_n}\mathbf{U})\,dS=0. \tag{7}$$

Within each triangular element or control volume, $\mathbf{U}$ is assumed to be constant and the flux across each edge, j of the element, i is determined by the states in the neighbouring elements separated by edge j. Discretising (7), the basic equation for the finite volume method becomes

$$A_i \frac{d\mathbf{U}_i}{dt} + \sum_{j \in N(i)} \mathbf{T}^{-1}_{\mathbf{n}_{i,j}} \widetilde{\mathbf{G}}(\mathbf{T}_{\mathbf{n}_{i,j}} \mathbf{U}_i, \mathbf{T}_{\mathbf{n}_{i,j}} \mathbf{U}_j) L_{i,j} = 0 \tag{8}$$

where A_i is the area of the element i, $N(i)$ is the set of all elements which share a common edge with element i, $L_{i,j}$ is the arc length of the edge between element i and element j and $\widetilde{\mathbf{G}}(\mathbf{T}_{\mathbf{n}_{i,j}} \mathbf{U}_i, \mathbf{T}_{\mathbf{n}_{i,j}} \mathbf{U}_j)$ is an estimate of the flux across the boundary separating two neighbouring elements. The major advantages of this formulation are;

1. The underlying principle is simple.
2. The ability to use flexible meshes, such as triangles or quadrilaterals which suit problems with complex geometries.
3. The use of an integral conservation law such that the solution may be smooth or discontinuous.

4.1 Solution of the One-Dimensional Riemann Problem

In (8), an estimate of the normal outward flux, $\widetilde{\mathbf{G}}(\mathbf{T}_{\mathbf{n}_{i,j}}\mathbf{U}_i, \mathbf{T}_{\mathbf{n}_{i,j}}\mathbf{U}_j)$ is required. With an appropriate rotation so that the outward normal coincides with the x-direction, then $\mathbf{U}_l = \mathbf{T}_{\mathbf{n}_{i,j}}\mathbf{U}_i$ and $\mathbf{U}_r = \mathbf{T}_{\mathbf{n}_{i,j}}\mathbf{U}_j$. The problem now involves the solution of a local one-dimensional problem in the direction normal to the element interface, where $\mathbf{U}_l$ and $\mathbf{U}_r$ are the states in neighbouring elements with common boundaries. Recalling that within each cell $\mathbf{U}$ is constant, then this will usually result in a discontinuity across the edge between elements E_i and E_j.

There are a number of schemes that can be used to define this flux. A wide range of numerical schemes have been examined for the solution of the one-dimensional shallow water equation applied to problems with discontinuities in the solution. Although many numerical schemes satisfy the *Rankine-Hugoniot jump condition* for shocks, they produce entropy violating shock solutions. For example, some first-order upwind schemes [2], [10], [16] exhibit problems with sonic points at the transition from subcritical to supercritical flow. This entropy violating solution is due to the inability of first-order upwind scheme to establish the direction of the flow at a point with zero horizontal momentum (this corresponds to the problem observed at sonic points in compressible flow dynamics). Other numerical schemes produce more dramatic discontinuities in the simulated profiles.

Only approximate Riemann solvers which either explicitly or implicitly include sonic points in estimating the intercell flux avoid the entropy violating solution. These include Osher's P scheme [4] and the scheme recently developed by Toro [12], [5]. This scheme implicitly includes sonic points. We use Toro's scheme as our approximate Riemann solver

The approximate Riemann solver solves the following Riemann problem

$$\mathbf{U}(x,0) = \begin{cases} \mathbf{U}_l & \text{If } x \geq 0 \\ \mathbf{U}_r & \text{If } x < 0. \end{cases} \tag{9}$$

where l and r denote the states on either side of a discontinuity. The Riemann problem can be decomposed into three waves for the two-dimensional shallow water equations. The middle wave is always a contact discontinuity and the left and right waves can be either shocks or rarefaction waves. Classic approximate Riemann solvers assume that the solution of (9) consists of only two waves separating three constant state regions. For the one-dimensional shallow water equation this is correct. For the two-dimensional shallow water equation however, there is a third wave, which is a contact discontinuity. Toro *et al.* [14] developed an approximate Riemann solver that includes the contact discontinuity in the solution.

Given the initial data; h_l, h_r, u_l, u_r, v_l and v_r, the Riemann problem for the two-dimensional problem has the structure shown in Figure 1 of four constant states separated by shocks or rarefaction fans to the left, centre and right with speeds S_l, S_m and S_r.

The solution for h and u is unaffected by v and the complete solution of

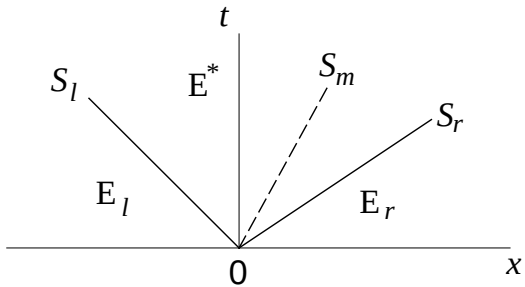

FIGURE 1: Structure of Solution of Riemann Problem: S_l and S_r are either shock or rarefaction waves and S_m is a contact discontinuity.

the Riemann problem for the conservative quantities, h and uh in the two-dimensional problem is identical to that required for the one-dimensional shallow water equation.

Toro's method provides estimates of the shock speeds

$$\begin{aligned} S_l &= \min(u_l - \sqrt{gh_l}, u^* - \sqrt{gh^*}) \\ S_r &= \max(u_r + \sqrt{gh_r}, u^* + \sqrt{gh^*}) \end{aligned} \tag{10}$$

where

$$u^* = \frac{u_l + u_r}{2} + \sqrt{gh_l} - \sqrt{gh_r} \tag{11}$$

and

$$h^* = \frac{(u_l + 2\sqrt{gh_l} - u_r - 2\sqrt{gh_r})^2}{16} \tag{12}$$

are the estimates of the h and u values of the intermediate state.

This is an explicit scheme with the usual Courant restriction on the time step. Here the restriction on the computational time step is $\Delta t c \leq \Delta x$ in which $c = \max(|S_l|_i, |S_r|_i \ \forall \ i)$ and Δx is the distance from the centroid of a triangle to the midpoint of the side of the triangle closest to the centroid. Although the solution may be smooth in some regions, the first-order approximate Riemann solver is solved at each cell interface. The solution of the Riemann problem will automatically establish whether the states on either side of a cell interface will degenerate into a shock or a smooth rarefaction fan.

4.2 Dry Bed Problem

Equation (10) assumes that there exists a finite water depth everywhere. If a dry bed exists upstream $h_l = 0$, the two eigenvalues collapse into one and the system of equations is not strictly hyperbolic. Under these circumstances no shock exists and S_l represents the speed of the head of the rarefaction wave and S_r represents the speed of the toe of the rarefaction wave. Therefore,

$$\begin{aligned} S_l &= u_r - 2\sqrt{gh_r} \\ S_m &= S_l \\ S_r &= u_r + \sqrt{gh_r}. \end{aligned} \tag{13}$$

Similar expressions can be derived for a dry bed downstream.

4.3 Limiters

Within each triangle the conserved quantities are assumed to be constant, see Figure 2(a). These values could be used to represent the left and right states between adjacent triangles. The use of these quantities in the Riemann solver will result in first-order approximations of the interface fluxes. In order to obtain second-order accuracy, a piecewise linear estimate of the left and right states is required. For a given cell, j the second-order approximation of the conserved quantities at the midpoint of the interface between elements E_i and E_j is expressed as

$$\mathbf{U}_l = \mathbf{U}_j + \nabla \mathbf{U}_j \cdot \mathbf{r}_j$$

where $\mathbf{U}_l$ is an estimate of the conserved quantities to the left of the continuity along the common edge, $\overline{AB}$ between triangles i and j, $\mathbf{r}_j$ is the vector from the cell centroid to the midpoint of $\overline{AE}$, $\mathbf{U}_j$ is the vector of conserved quantities at the centroid of triangle j and $\nabla \mathbf{U}_j$ is the gradient of triangle formed using the centroid values of all neighbouring triangles to triangle j, see Figure 2(b).

Numerical oscillations are common with second and higher-order numerical schemes. These oscillations can be controlled by either limiting them using non-linear limiters or by introducing artificial viscosity in the numerical scheme. Here, non-linear limiters are used during the estimation of conserved quantities at the edges of each element so that oscillations that would have introduced by new local extrema in the solution are suppressed. The *limiter*

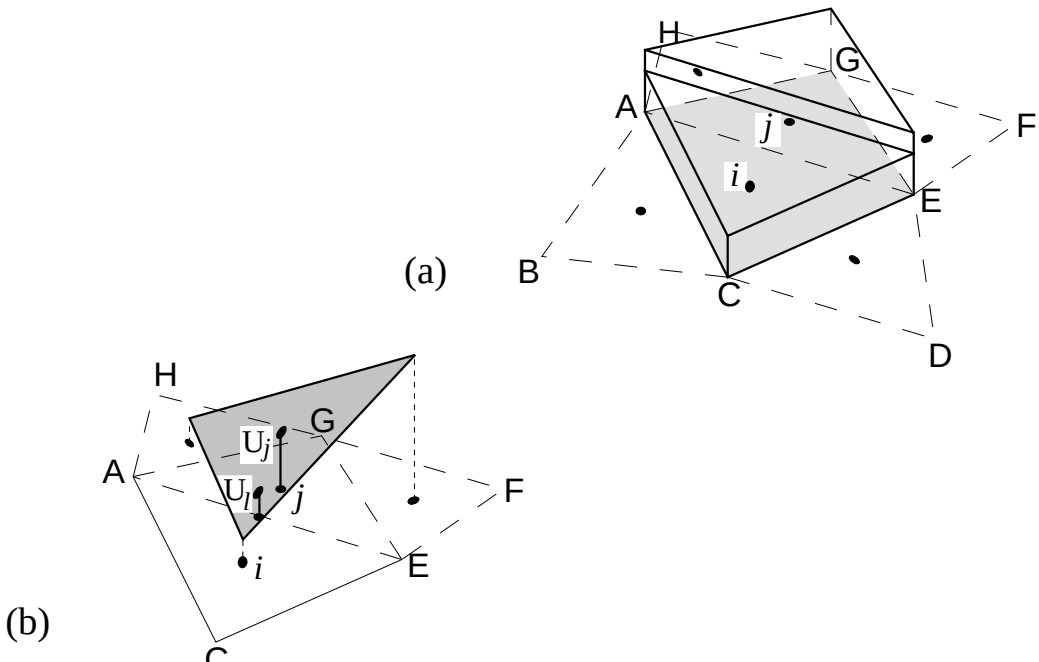

FIGURE 2: Triangular elements in the finite volume method.

is applied to the gradient terms so that

$$\mathbf{U}_l = \mathbf{U}_j + \Phi_j \nabla \mathbf{U}_j \cdot \mathbf{r}$$

where $0 \leq \Phi_j \leq 1$ is a chosen limiter. When Φ_j is set to zero, the computation domain is characterised by piecewise constant regions resulting in a first-order scheme. The non-linear limiter is given by

$$\Phi_j = \max\left[\min(\beta r_j, 1), \min(r_j, \beta)\right] \tag{14}$$

where

$$r_j = \begin{cases} (\mathbf{U}_j^{\max} - \mathbf{U}_j)/(\mathbf{U}_l - \mathbf{U}_j) & \text{If } \mathbf{U}_l > \mathbf{U}_j \\ (\mathbf{U}_j^{\min} - \mathbf{U}_j)/(\mathbf{U}_l - \mathbf{U}_j) & \text{If } \mathbf{U}_l < \mathbf{U}_j \\ 1 & \text{If } \mathbf{U}_l = \mathbf{U}_j \end{cases}$$

and

$$\mathbf{U}_j^{\min} = \min(\mathbf{U}_j, \mathbf{U}_i), \;\; \mathbf{U}_j^{\max} = \max(\mathbf{U}_j, \mathbf{U}_i).$$

This procedure is carried out sequentially for the two triangles separated by $\overline{AB}$ giving U_l and U_r. These are used in the Riemann solver to estimate the flux across $\overline{AB}$. When $\beta = 1$, Φ is the MINIMOD limiter and when $\beta = 2$ the limiter is Roe's SUPERBEE limiter. This approach is similar to that used by Anastasiou and Chang [1]. It differs from theirs because their limiter is defined as

$$\Phi = \min(\Phi_j), \qquad j = 1, 2, 3.$$

In this case there are circumstances which lead to very small values of h at the edges of a triangle. In addition it was possible for $U_i > U_j$ but for $U_l < U_r$. We added an extra amount of limiting to ensure that if $U_i > U_j$, then $U_l \geq U_r$. In addition we found it necessary to choose $\beta = 1$. Without these extra conditions very small values of h produced very large values for $u = uh/h$. To satisfy the Courant criterion extremely small time step are required by the explicit scheme. These extremely small time steps make the scheme computationally expensive. The new approach limits estimates of the dependent variables at each triangle edge by the values between adjacent triangles. This overcomes the problem of obtaining small values of h. The time steps that can be used in the dry bed problem remain competitive with implicit schemes, which require the solution of large systems of non-linear equations. Although, this is compensated for by the advantages of an unrestricted time step, for some problems the speed of the transients may only be adequately resolved with small time steps such as those commonly employed in explicit schemes.

4.4 Boundary Conditions

The boundary conditions are very simple to implement in this scheme. For a cell, with constant state $\mathbf{U} = [h\ uh\ vh]^T$ which has an edge that forms a boundary, then it is only necessary to specify the unknown state, $\mathbf{U}_b$ on the

other side of the boundary. For a transmissive boundary condition

$$\mathbf{U}_b = \mathbf{U} \tag{15}$$

and for a reflective boundary

$$\mathbf{U}_b = \begin{bmatrix} h \\ -uh \\ vh \end{bmatrix}. \tag{16}$$

5 Hypothetical Examples

The finite volume scheme is demonstrated using a problem containing 100 by 100 computational cells, each cell has a width of $\Delta x = 0.2$ metres. The initial conditions consist of two states separated by a circular discontinuity. The radius of the circle $r = 5$ metres and it is centred at $x = 0$ metres. Both components of the velocity u and v are set to zero everywhere and h is set to $h_1 = 10$ metres within the circle and (a) $h_0 = 1$ or (b) $h_0 = 0$ metres outside the circle. In the computational scheme, $\Delta t = 0.005$ seconds, which satisfies the Courant criterion, $Cr = w\Delta t/\Delta x \leq 1$, where $w = \sqrt{u^2 + v^2}$ and the solution is sought when $t = 0.15$ seconds. In case (a), by time $t = 0.15$ seconds, a bore has formed. Fluid drains from the deepest region as a rarefaction wave progresses outwards. In this region supercritical flow exists. The results for the second-order finite volume scheme are shown in Figure 3(a). Figure 3(b) shows the solution when $h_0 = 0$, the dry bed case.

We see that no bore forms, instead a rarefaction wave extends into the dry bed. The finite volume scheme produces sharp resolution of the shock and discontinuities.

6 Conclusion

A model capable of simulating unsteady two-dimensional unsteady flow on an arbitrary triangular grid is described. The second-order finite volume scheme is comparable to second-order schemes solved on Cartesian grids. However, it avoids the generation of secondary waves associated with Cartesian grids. It is also capable of handling the dry bed problem without generating large velocities.

References

[1] K. Anastasiou and C.T. Chan. Solution of the 2D shallow water equations using the finite volume method on unstructured triangular meshes. *International Journal for Numerical Methods in Fluids*, 24(11):1225–1245, 1997. C1264, C1274

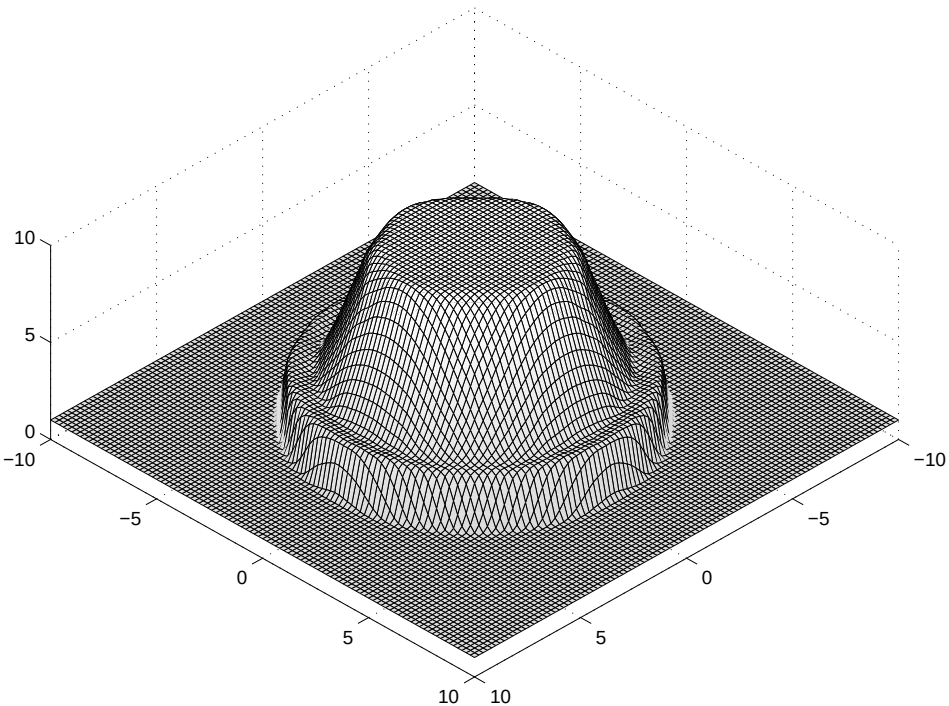

FIGURE 3: (a) Two-dimensional solution of the circular dam break problem using our finite volume scheme. Solution at time $t = 0.15$ with initial conditions consisting of a plug of water of radius 5 metres and height h_1 in a pond of water of depth h_0: $h_0 = 1m$ and $h_1 = 10m$.

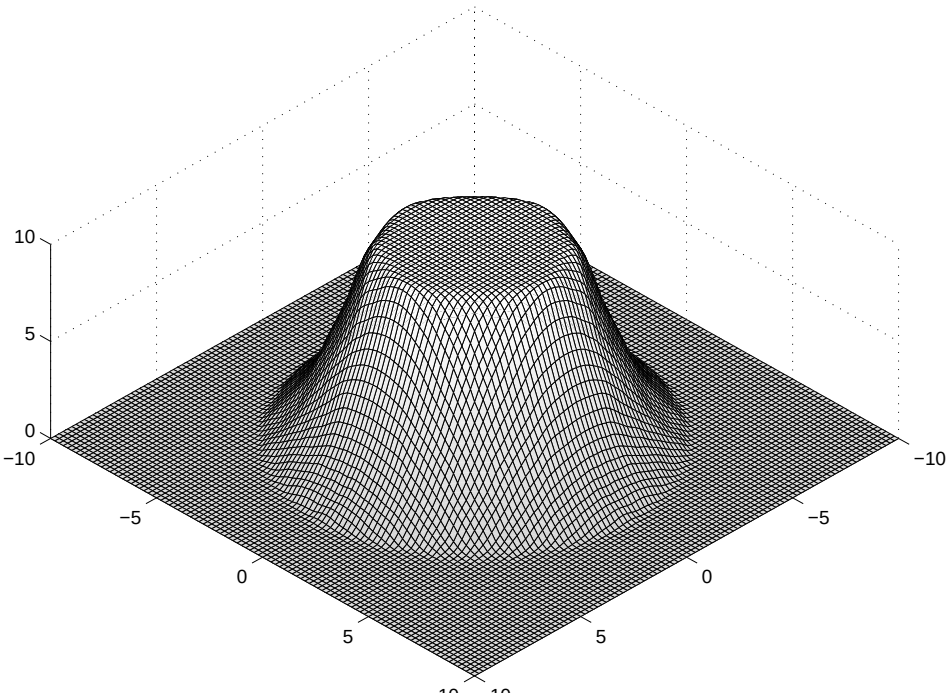

FIGURE 3: (b) $h_0 = 0m$ and $h_1 = 10m$.

[2] A. Bermudez and M.E. Vazquez. Upwind methods for hyperbolic conservation laws with source terms. *Computers Fluids*, 23(8):1049–1071, 1994. C1268

[3] S.J. Billett and E.F. Toro. On WAF-type schemes for multidimensional hyperbolic conservation laws. *Journal of Computational Physics*, 130(1):1–24, 1997. C1264, C1264

[4] B. Engquist and S. Osher. One sided difference approximations for nonlinear conservation laws. *Mathematics of Computation*, 36(154):321–351, 1981. C1264, C1269

[5] L. Fraccarollo and E.F. Toro. Experimental and numerical assessment of the shallow water model for two-dimensional dam-break type. *Journal of Computational Physics*, 33(6):843–864, 1995. C1264, C1269

[6] C. Hirsch. *Numerical Computation of Internal and External Flows, Volume 1, Fundamentals of Numerical Discretization*. John Wiley and Sons, New York, 1988. C1265

[7] C.G. Minghan and D.M. Causon. High resolution finite-volume method for shallow water flows. *Journal of Hydraulic Engineering, American Society of Civil Engineers*, 124(6):605–614, 1998.

[8] S. Osher and F. Solomon. Upwind difference schemes for hyperbolic conservation laws. *Mathematics of Computation*, 38(158):339–374, 1982.

[9] P.L. Roe. Approximate Riemann solvers, parameter vectors, and difference schemes. *Journal of Computational Physics*, 43(3):357–372, 1981. C1264

[10] J.L. Steger and R.F. Warming. Flux vector splitting of the inviscid gas dynamic equations with application to finite-difference methods. *Journal of Computational Physics*, 40(2):263–293, 1981. C1268

[11] G. Strang. On the construction and comparison of finite difference schemes. *Society for Industrial and Applied Mathematics, Journal for Numerical Analysis*, 5(3):506–517, 1968. C1264

[12] E.F. Toro. A weighted average flux method for hyperbolic conservation laws. *Proceedings of the Royal Society*, Series A, 423:401–418, 1989. C1265, C1265, C1269

[13] E.F. Toro. Riemann problems and the WAF method for solving the two-dimensional shallow water equations. *Philosophical Transactions of the Royal Society, London*, Series A, 338:43–68, 1992. C1262

[14] E.F. Toro, M. Spruce and W. Speares. Restoration of the contact surface in the HLL-Riemann solver. *Shock Waves*, 4:25–34, 1994. C1269

[15] T. Weiyan. *Shallow Water Hydrodynamics: Mathematical Theory and Numerical Solution for Two-Dimensional System of Shallow Water Equations*. Elsevier Science Publishers, 1992. C1263

[16] J.Y. Yang, C.A. Hsu and S.H. Chang. Computations of free surface flows Part 1: One-dimensional dam-break flow. *Journal of Hydraulic Research*, 31(1):19–34, 1993. C1268

[17] D.H. Zhao, H.W. Shen, G.Q. Tabios, J.S., Lai, and W.Y. Tan. Finite-volume two-dimensional unsteady-flow model for river basins. *Journal of Hydraulic Engineering, American Society of Civil Engineers*, 120(7):863–883, 1994. C1264

[18] C. Zoppou and S. Roberts. Catastrophic collapse of water supply reservoirs in urban areas. *Journal of Hydraulic Engineering, American Society of Civil Engineers*, 125(7):686–695, 1999.